LA-UR- 96-1932

CONF-960610--14

Title: MULTI-KILOAMPERE, ELECTRON-BEAM GENERATION USING METAL PHOTO-CATHODES DRIVEN BY ArF AND KrF LASERS

RECEIVED
JUL 19 1996
OSTI

Author(s): R. L. Carlson, S. A. Moya, R. N. Ridlon, G. J. Seitz, R. P. Shurter

Submitted to: High Power Particle Beams, Prague, June 1996

Los Alamos
NATIONAL LABORATORY

Multi-Kiloampere, Electron-Beam Generation using Metal Photo-Cathodes Driven by ArF and KrF Lasers*

Randolph L. Carlson, Steven A. Moya, Rae N. Ridlon, Gerald J. Seitz, and Roger P. Shurter

Los Alamos National Laboratory, Los Alamos, New Mexico, 87545, USA

Abstract

An electron-beam-pumped laser operating at ArF (193 nm) or KrF (248 nm) producing 35 MW (3.5 J in 100 ns) has been used to illuminate a micro-machined aluminum cathode. The cathode was pulsed to 2.75 MV at fields of 185 kV/cm (15-cm AK gap) using REX [1,2] (a 4-MV, 5-kA, 85-ns) pulsed-diode machine. The extracted current versus incident laser power; and therefore, quantum efficiency was measured for KrF at $5x10^{-5}$; ArF was significantly higher at $1x10^{-3}$. Current densities of 100 A/cm^2 and total currents of 2 kA have been achieved, the latter by increasing the cathode area in proportion to the laser power.

Introduction

A laser-driven photo-injector was first demonstrated [3] in 1985; afterwards, others [4-9] used available high power ArF and KrF lasers to pursue higher currents from the irradiation of simple metals via the photoelectric effect. These technologies presently provide the only known methods to reduce significantly the cathode source temperature and therefore, the emittance of present and future multi-kA injectors. Our present work is significant in that the cathode exists in the presence of outgasing materials with a background vacuum pressure in the mid 10^{-6} torr regime and 100-ns-long electron beams of several kA have been produced.

The quantum efficiency, QE, is defined in this paper as: QE = (I/P)(#eV/photon) where I is the emitted beam current, P is the laser power incident on the cathode, and the energy/photon is 5 and 6.4 eV for KrF and ArF, respectively. A companion paper [10] reports the results of small-scale, short-pulse ArF studies to further address the relative quantum efficiencies of other candidate metals, their preparation, and the effects of vacuum and mono-layer contaminants.

Table 1 lists typical properties of four materials suitable for a cathode [11,12]; micro-machined Aluminum alloy 6061-T6 was chosen for this work based upon our previous results [6-9]. The potential for laser damage to these materials was assessed by a calculation; the surface temperature rise is shown in Fig. 1 for an absorbed laser intensity, F, of 1 MW/cm^2. The experimental laser pulse is shown overlaid with a trapezoidal fit (45-ns rise, 75-ns flattop, 125-ns fall) used to determine the temperature rise. The calculation of the surface temperature, T(z,t), follows the methods of Ready [13] using the parametric integral:

$$T(z,t) = k^{1/2}/(K\pi^{1/2}) \int_0^t \tau^{-1/2} F(t-\tau) \exp(-z^2/4k\tau) d\tau,$$ which has an analytic solution for a ramp of slope F/tp at z = 0 given by $T(0,t) = (4/3K)(F/tp)(k/\pi)^{1/2} t^{3/2}$. The surface temperature profiles in the plot were obtained by using the ramp solution to make a piecewise trapezoid. Since T(0,t) is proportional to $k^{1/2}/K = 1/(\rho CpK)^{1/2}$ this parameter is also listed in Table 1. Magnesium reaches the highest (220°C); diamond is a factor of four lower at (55°C). When the first phase change of diamond is considered, its laser damage threshold could be ~20 times that of magnesium.

*Work performed under the auspices of the U.S. Department of Energy.

Table 1. Properties of Some Cathode Materials.

	Mg	Al	Cu	Diamond
K (W/cm°C)	1.59	2.37	3.98	23.1
k (cm^2/sec)	0.90	1.06	1.17	12.7
Cp (J/gm°C)	1.02	0.83	0.38	0.52
ρ (gm/cm^3)	1.74	2.70	8.96	3.52
ρ*Cp*K	2.81	5.31	13.55	42.0
Tmp(°C)	649	660	1083	~3550
WF (eV)	3.68	4.08	4.52	5.50

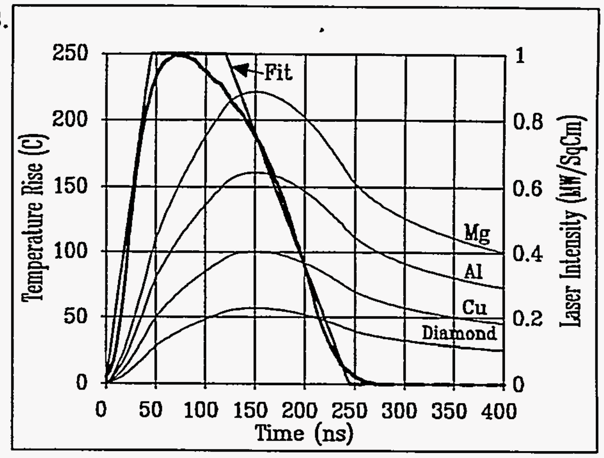

Figure 1. Material Temperature Rise.

Experimental Test Setup

Figure 2 shows the layout of the REX Facility, E-beam diode head region, excimer laser diode with beam paths, and diagnostics. For QE measurements at normal incidence, the laser beam was directed by a turning mirror to a 20-cm-diam lens (f = 415 cm) and focused through a window and onto the REX cathode. Nitrogen purged beam pipes were used to reduce the appreciable attenuation of ArF due to oxygen. The laser light was monitored by vacuum photodiodes at the source (SAM PD) and cathode (REX PD); a gated photo-multiplier was used to record visible light emission from the cathode. The energy and spatial profile of the beam were recorded at the cathode conjugates by an Energy Monitor (Pyrex based, Scientech Inc., 10-cm absorbing calorimeter) and a Profile Monitor (Star Tech Instruments Inc., BIP-3100/Z6/F100, 10-cm, UV to CCD converter). Beam current was monitored at the anode and at the test section entrance (205 cm from the cathode) with beam size and position adjusted at this location by the anode extraction magnet and x-y steering coils, respectively. The AK gap voltage was monitored by an array of four, integrated E-Dots flush-mounted on the anode face; these were cross-calibrated by an energy spectrometer. Initial beam temperature and QE measurements at 60 degrees incidence used the alternate laser beam path as shown. Beam temperature diagnostics included a Beam and Scintillator Mask as in [1,9] with an optical path to a shielded screen room.

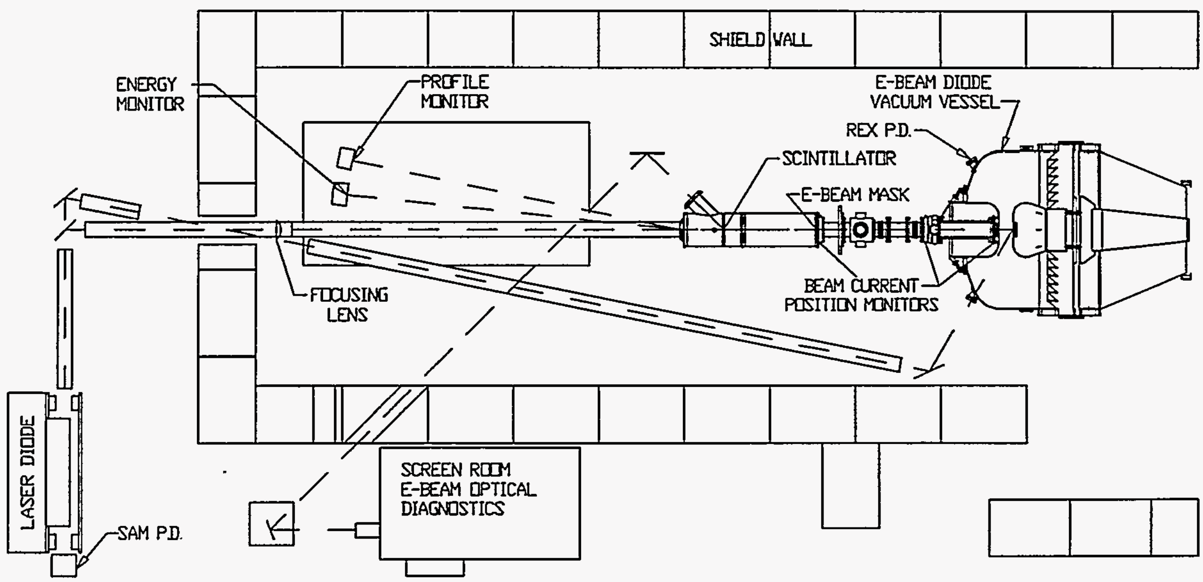

Figure 2. Layout of REX Electron-Beam Facility with Excimer Laser Diode.

Results

Figure 3 shows the voltage/current (VI) characteristics of a 6.35-cm-diam velvet cathode with the calculated [14] space-charge-limited (SCL) current plotted in Fig. 4. REX produces both a primary and lower secondary pulse, the latter proved useful to study any late time emission from the cathode. As in Ref. 1, a coefficient following the energy scaling of Jory-Trivelpiece was fit to the points in Fig. 4. The current for cathode radius, Rc, and AK gap, d, is given by $C(\gamma^{1/2} - 0.8471)^2(Rc/d)^2$ kA where the fit is $C = 46.7 - 11.8(Rc) + 1.15(Rc)^2$. At 2.6 MV this expression over predicts by 10% the current to be 2.45 kA versus the 2.18 kA measured.

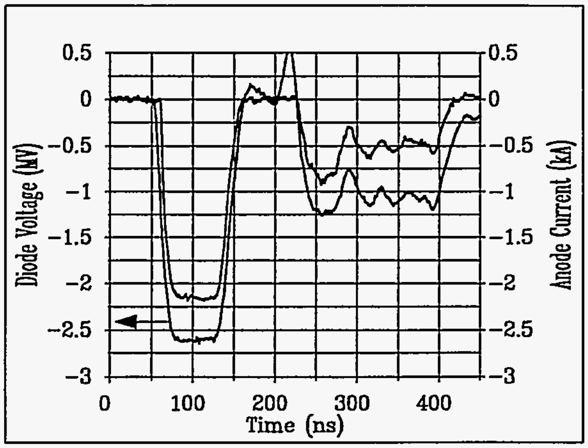

Figure 3. VI Characteristics of 6.35-cm-diam Velvet Cathode at 2.6 MV; AK Gap is 15 cm.

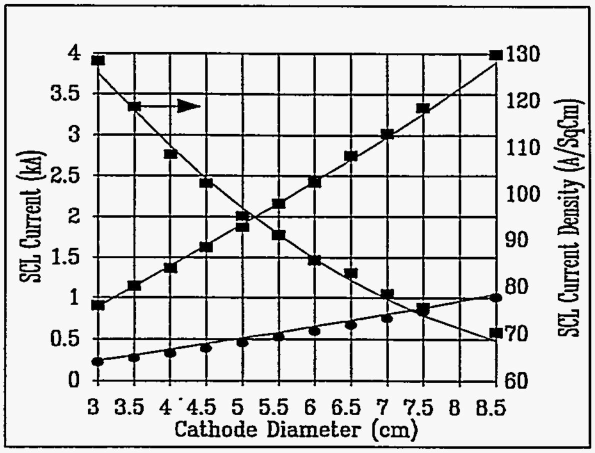

Figure 4. Calculated SCL Current at 2.75 MV (■) and 1.0 MV (●); AK Gap is 15 cm.

Figure 5 shows the anode current, diode voltage, and REX PD for a laser power of 8.3 MW under emission limited (current follows REX PD) conditions. As the laser power was increased to 11.6 MW, the current approached the SCL regime (current follows voltage) as in Fig. 6. The laser beam had a $1/e^2$ diameter of 6.5 cm; however, the effective beam area was smaller for the 'parabolic' type profile of Fig. 7(b). The fit of Fig. 4 gives a 90% SCL current of 1.95 kA for a 5.5-cm-diam cathode in good agreement with the beam effective 5.3-cm-diam. Figure 7(a) shows the near 'top-hat' beam used for the lower power (< 8 MW) 5.5-cm-diam tests.

The anode current versus laser power for three different Al samples and two beam sizes are plotted in Fig. 8 with QE fits for ArF and KrF. Although the cathodes were diamond turned

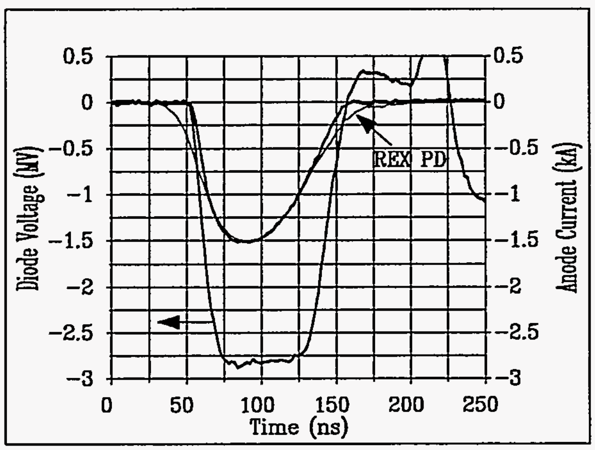

Figure 5. VI of Photo-Cathode at 8.3 MW.

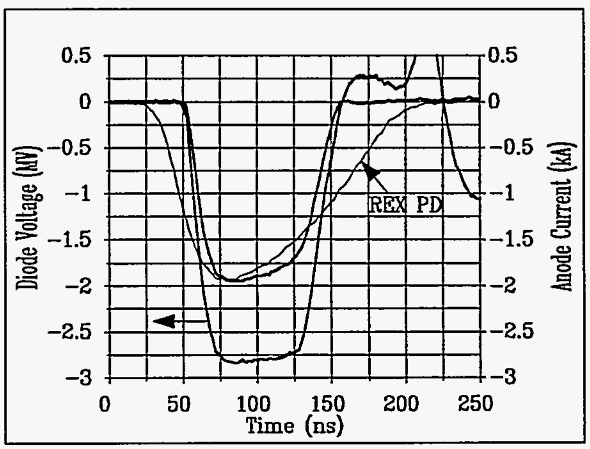

Figure 6. VI of Photo-Cathode at 11.6 MW.

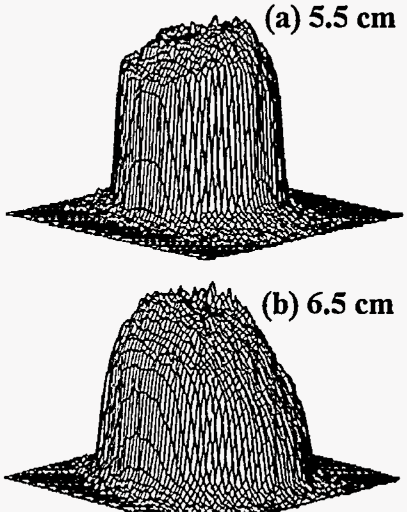

Figure 7. ArF Beam Profiles.

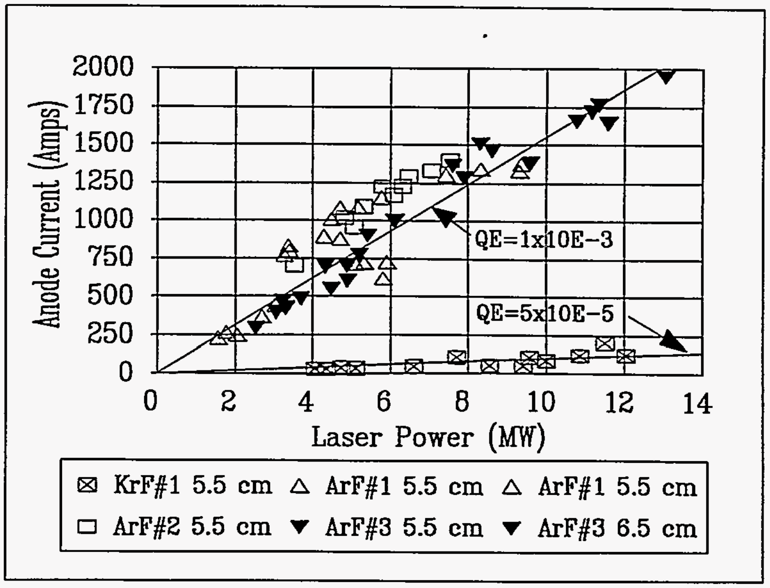

Figure 8. Anode Current vs Laser Power for Al 6061-T6.

mirror surfaces, small (~0.1 to 1 mm) damage sites developed over less than 1% of the area after tens of shots. This was not expected at even the highest peak laser intensities (~0.85 MW/cm^2) since low temperature rises were predicted [Fig. 4]. These damage sites may be at inclusions of magnesium and silicon in the alloy. Initially, post-laser field emission occurred during the second pulse of REX [Fig. 3] but this gradually went away after apparent conditioning of the sample [Figs. 5,6]. Visible light tracked the laser light on the cathode. A limited set of KrF data was taken since QE's ~5×10^{-5} agree with previous work [7-9] and higher ArF QE's ~1×10^{-3} are of more practical interest. Figure 8 may suggest higher QE's due to sample conditioning and weak multi-photon processes at higher intensities when near-SCL data points are ignored. Initial results at 60 degrees normal incidence gave ~35% lower ArF QE's probably due to increased sample reflectivity; this might be increased by micro-grooving the cathode surface [12].

In summary, current densities of 100 A/cm^2 and total currents of 2 kA have been achieved for 100-ns-long ArF laser pulses on aluminum. By increasing the laser power per unit area, space charge limited operation has been demonstrated at 1.25 kA. Higher quantum efficiencies might be attained by using 1:1:1 diamond films [11] and a diamond-based cathode should also be more robust against laser damage. Beam temperature measurements are underway.

[1] T.P. Hughes, R.L. Carlson, and D.C. Moir: J.Appl.Phys. **68** (6), (1990), pp. 2562-2571.
[2] R.L. Carlson, et al: Proc. of the *1991 IEEE Pulsed Power Conference*, pp. 82-85.
[3] J. Fraser and R. Sheffield: Nucl.Instr.&Meth. A250, (1986), pp. 71-76.
[4] S.W. Downey, et al: Appl.Phys.Lett. **49** (15), (1986), pp. 911-913.
[5] J.D. Saunders, T.J. Ringler, et al: Proc. of the *1987 IEEE Particle Accelerator Conference*, pp. 337-339.
[6] Thomas J. Ringler: THESIS, Naval Postgraduate School, Monterey, CA, September, 1987.
[7] T.J. Kauppila, et al: Proc. of the *1987 IEEE Particle Accelerator Conference*, pp. 273-275.
[8] T.J. Kauppila, et al: Proc. of the *1989 IEEE Particle Accelerator Conference*, pp. 322-324.
[9] T.J. Kauppila, R.L. Carlson, et al: Proc. of the *1991 IEEE Particle Accelerator Conference*, pp. 2107-2109.
[10] R.P. Shurter, et al: paper at this conference.
[11] J. Fischer, T. Srinivasan-Rao, T. Tsang, and G. Brandes: Nucl.Instr.&Meth. A340, (1994), pp. 190-194.
[12] T. Tanabe, Y. Kawamura, D. Li, and K. Toyoda: Rev.Sci.Instrum. **66** (2), (1995), pp. 1010-1014.
[13] J.F. Ready: "Effects of High Power Laser Radiation," Academic Press, New York, (1971), p. 73, (eqs: 3.8, 3.9).
[14] PBGUNS Code run by T.P. Hughes of Mission Research Corp., developed by J. Boers: Proc. of the *1993 IEEE Particle Accelerator Conference*, (1993), pp. 327-332.